Original Research Article **Biomaterial**

International Journal of Pharma and Bio Sciences

ISSN 0975-6299

ANTIBACTERIAL EVALUATION OF SOFT AND HARD COATINGS FOR BIOMEDICAL APPLICATIONS

SUGANTHAN VEERACHAMY [A, B], GEETHA MANIVASAGAM* [B, C]

[a.] School of Electronics and Engineering [SENSE], VIT University, Vellore 632014
[b.] Centre for Biomaterials, Cellular and Molecular Theranostics [CBCMT], Vellore 632014
[c.] School of Mechanical Engineering [SMEC], VIT University, Vellore 632014

ABSTRACT

This paper reports on the mechanical, microstructure, phase analysis and antibacterial activity of two different wear-resistant and osseointegration coatings performed on Ti-6Al-4V alloys for orthopedic applications. The powders of following compositions were sprayed using atmospheric plasma spray process onto Ti-6Al-4V alloy a) alumina-titania, [AT] b) yttrium stabilized zirconia [YSZ], c) bilayered AT/YSZ, d) bilayered YSZ/AT, e) Hydroxyapatite [HaP], f) TiO_2 g) HaP [30%] + TiO_2 [70%], h) HaP [70%] + TiO_2 [30%] and i) HaP [50%] + TiO_2 [50%]. The coatings were characterized using X-ray diffraction (XRD), Scanning electron microscope (SEM) and surface roughness measurement. In addition, microindentation hardness measurements and scratch strength measurements were also performed. Amongst the various coatings AT, BL AT/YSZ and 3H7T exhibited higher hardness values and BL YSZ/AT and 3H7T offered higher scratch resistance. Antibacterial testing was also performed on all the coatings. The wettability studies reveal the soft coating to be hydrophilic and hard coating as hydrophobic. Comparatively, there were less *S. aureus* on plasma sprayed soft coatings deposited on Ti-alloys compared with hard coatings after 18 hours of culture respectively. From the results, 3H7T, AT and BL AT/YSZ have less number of bacterial colonies adhered to its surface.

KEYWORDS: **Hard coatings, soft coatings, plasma spraying, wettability, antibacterial studies.**

GEETHA MANIVASAGAM*
Centre for Biomaterials, Cellular and Molecular Theranostics [CBCMT], Vellore 632014
School of Mechanical Engineering [SMEC], VIT University, Vellore 632014

Received on : 18/10/2016,
Revised and Accepted on 10-12-2016
DOI: http://dx.doi.org/10.22376/ijpbs.b358-369

INTRODUCTION

Ti-6Al-4V is one of the widely used implant material because of their highly advantageous properties such as low density, biocompatibility and high strength to weight ratio. Ti-6Al-4V exhibits superior corrosion resistance because of the formation of a highly stable oxide film on its surface on exposure to air. The thickness of the oxide film is about 10µm and protects the bulk material from corrosion. However, Ti-6Al-4V also suffers from poor wear resistance and hence in the presence of body fluids and protein complexes in human body might lead to disruption/diffusion of the oxide layer and hence, aggravate corrosion process. The conjoint action of both wear and corrosion leads to release of wear debris in the peri-implant region and activates a cascade of immune response which leads to the activation of osteoclast cells and hence, osteolysis of the peri-implant region resulting in implant loosening [1]. In addition, on long-term application, the leached out metal ions has also been found to be carcinogenic. Hence, it is of utmost importance to prevent the release of the debris after implantation. In addition to aseptic loosening, infection is also considered to be one of the main reasons for implant failure. *Staphylococcus aureus* is a Gram positive coccal bacterium and has been found to be the cause of major orthopedic infections [2]. Once the bacteria adhere on the implant site, it tends to form a biofilm by production of extracellular polysaccharides. Biofilms can obstruct immune response and are also highly resistant to systemic antibiotic therapy thereby, resulting in chronic infections [3]. To overcome revision due to infection, attempts have been made to develop coatings with antibacterial property[4, 5, 6, 7]. Apart from the above mentioned reasons for failure of Ti implant, the other disadvantage of metallic implant is they are bioinert and hence does not induce bone formation on the surface. Often HaP is coated on metallic implants as it possesses composition similar to bone and hence induce osteoinduction. Thus surface modification of metallic implants is the only solution to overcome all the challenges mentioned with regard to metallic implants. Various coating techniques such as electrophoretic deposition, dip coating, spin coating, pulsed laser deposition (PLD) and thermal spray process are used to prevent failure of Ti-6Al-4V. Among the above mentioned coating techniques, plasma spraying is extensively used in medical industry to deposit HaP due to enhanced bone formation, faster deposition rate, superior adhesion strength and higher coating thickness. In general, coatings based on the hardness are categorized into hard and soft coatings. Hard coating such as aluminia-titania (AT) and yttrium stabilized zirconia (YSZ) are employed for high wear resistant applications such as in case of total hip replacements due to their superior hardness, chemical inertness and higher resistance to abrasion and erosion. On the other hand, the main function of soft coatings involving Hydroxyapatite (HaP) and titanium dioxide (TiO_2) is to promote healing and bone growth. Hydroxyapatite (HaP), calcium phosphate crystal has been widely used to coat implant materials due to its superior biocompatibility and osteoconductivity properties. HaP coating has been found to result in more rapid fixation, stronger bonding and increased bone growth at the interface. Similarly, TiO_2 is used as a coating to enhance the corrosion resistance. The thermal expansion coefficient of HaP (13.6×10^{-6}/K), is much higher than that of Ti alloy substrate (8.7×10^{-6}/K), this results in the formation of cracks in coatings. Hence, coating HaP with TiO_2 would not only prevent corrosion but also helps to produce stable coatings as TiO_2 has relatively lower thermal expansion coefficient (7.249×10^{-6}/k). [8]. Further, the concentration of TiO_2 required to be added with HaP in order to have effective result is still unexplored and this motivated to carry the present work. Further, in spite of the fact there are several reports on coatings there are no systematic investigations on the antibacterial behaviour of such coatings. The applications of wear resistant hard coatings and osseointegration soft coatings are depicted in fig. 1.

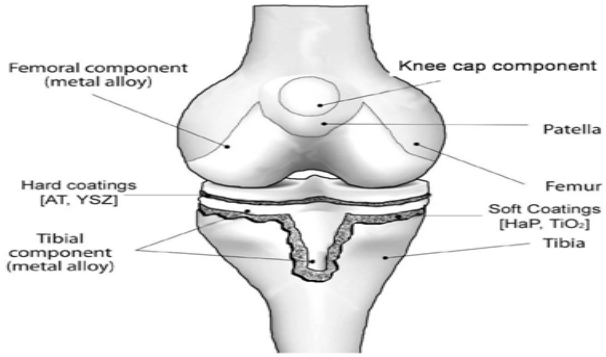

Figure 1
Schematic of wear-resistant hard and osseointegration soft coating with its applications

In the present study, an attempt was made to develop hard coatings consisting of AT - YSZ [alumina-titania & yttrium stabilized zirconia as mono and bilayered coatings] and soft HAP – TiO_2 composite coatings on Ti-6Al-4V substrate using atmospheric plasma spraying process. Different concentrations of HaP and TiO_2 [30%HaP+70%TiO_2 (3H7T), 70%HaP+30%TiO_2 (7H3T), 50%HaP+50%TiO_2 (5H5T)] were employed to prepare the composites and their phases and microstructure analysis, wettability and mechanical studies were investigated in detail. In addition, thorough investigations were performed to understand the effect of composition, wettability and roughness on the

antibacterial activity of the coatings which are commonly employed on biomedical implants.

MATERIALS AND METHODS

Plasma spraying of particles

Commercially available alumina 13WT% titania (AT) powder with particle size of 15-55µm and 8% yittrium stabilized zirconia (YSZ) with the similar particle size was purchased from *Inframat Corp*oration, USA and was used to obtain the composite feed stock powders for plasma spraying to develop mono and bilayered (AT/YSZ & YSZ/AT) hard coatings as shown in *fig.2*. On the otherhand for soft coatings, Hydroxyapatite (HaP) and TiO_2 powders were synthesized by a protocol developed by our group and reported elsewhere [9, 10] and its different compositions [30%HaP+70%TiO_2 (3H7T), 70%HaP+30%TiO_2 (7H3T), 50%HaP+50%TiO_2 (5H5T)] is shown in *fig.3*.

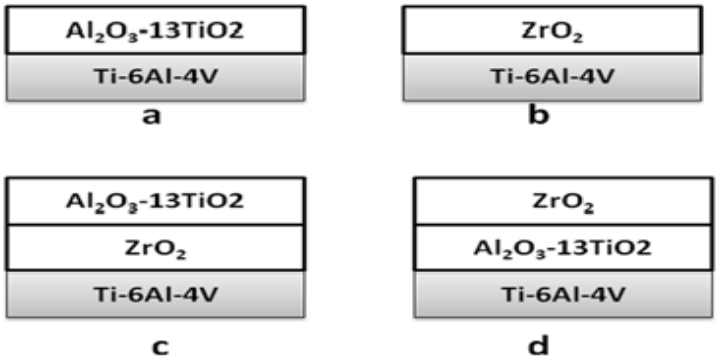

Figure 2
Schematic diagrams of (a) AT coating, (b) YSZ coating, (c) Bilayer – AT/YSZ coating, (d) Bilayer – YSZ/AT coating

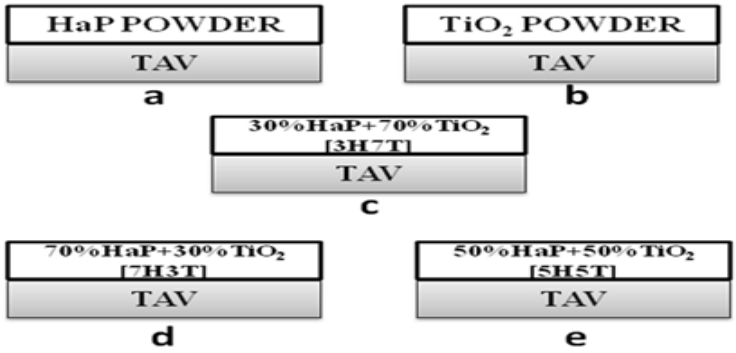

Figure 3
Schematic diagrams of a) HaP coating b) TiO_2 coating c) 3H7T coating d) 7H3T coating e) 5H5Tcoating

Plasma spraying of the powders on annealed Ti-6Al-4V rod [as per ASTM 348] with dimensions 10mm x 10mm x 5mm was carried out using 80kW plasma spray system (Sulzer Metco 9MB) . The specimens were mirror polished with SiC paper [800-2500 grits], followed by diamond polishing using 1µm diamond paste prior to plasma spraying. To remove contamination, the samples were washed with distilled water and ultrasonically cleaned in acetone for 10mins at 400°C. Prior to plasma spraying, the samples were preheated by means of the plasma torch, in order to enhance the adhesion of the coating. Depending upon the different melting temperature of powders used in the coatings, various process parameters have been employed for both hard and soft coatings and it is tabulated in *table 1 and 2* respectively.

Table 1
Plasma spray parameters used for plasma spraying AT and YSZ powders [monolayer and bilayer coating]

Parameters	AT coating	YSZ coating
Plasma current [A]	600	450
Plasma Voltage [V]	50	55
Ar gas flow pressure [NLPM]	42	42
H2 gas flow pressure [NLPM]	9	8
Carrier gas flow rate [psi]	45	45
Powder feed rate [g/m]	45	45
Spray distance [cm]	10	10

Table 2
Plasma spray parameters for HaP, TiO_2, 3H7T, 7H3T and 5H5T.

Parameters	HAP	TiO_2
Plasma current [A]	500	500
Plasma Voltage [V]	40	75
Ar gas flow pressure [NLPM]	50	80
H2 gas flow pressure [NLPM]	30	120
Carrier gas flow rate [psi]	45	45
Powder feed rate [g/m]	35	35
Spray distance [mm]	127	100

Characterization

Microstructure and Phase Analysis

The surface morphology of hard and soft composite coatings was observed by scanning electron microscope. Further, the objective of performing the XRD studies on the coating was to examine the possible phase transformation which the particles have undergone as they were taken to the molten state and quenched during the plasma process, which obviously would have a strong bearing on the mechanical properties of the powder and coatings. Phase analysis of the as-sprayed composite powders (AT & YSZ) and composite coatings (HaP & TiO_2) were performed using X-ray diffractometer (BRUKER-binary V2) with Cu Kα radiation. The current and voltage were set at 40kV and 30mA and all the readings were collected in the 2θ range from 10˚ to 80˚ in a step scan mode with a step of 2˚/min.

Hardness and Scratch Testing

Micro indentation hardness values were measured using Vickers micro hardness tester, across the polished cross-section of the as-sprayed composite using a load of 200g for 15s and the hardness values were measured at five different points and its average value is reported. The average surface roughness of the monolayered and bilayered coatings was measured using Talysurf CCI profilometer (Taylor Hobson). Scratch test was performed using a commercial micro scratch tester (DUCOM, India) to understand the scratch behavior of the AT: YSZ bilayered and HAP: TiO_2 composite coatings. In order to evaluate the adhesion strength of the hard and soft coatings, a scratch test with progressive loading from 0 to 100N was performed. A diamond stylus of 200µm radius was used to produce the scratch. The loading was varied in steps at 2 N/mm. The Scratch tracks were observed through optical microscope.[11]

Wettability

Contact angle measurements for surface wettability using the sessile drop technique were carried on the AT, YSZ, BL AT/ YSZ, BL YSZ/AT coatings and composite coatings of HaP: TiO_2 by a water droplet contact angle-based test (VCA optima, AST) according to the ASTM D7334-08 standard. A 1±0.1µL drop of water was utilized on the sample surface to measure the contact angles in a specified time (5 s). The test was repeated for five times for each of the samples.

Antibacterial Testing

Anti-bacterial assay was performed using *Staphylococcus aureus* (MTCC 8291) and the culture was maintained in nutrient broth (Himedia). A single colony was inoculated into 5 ml of sterile broth and incubated at 37℃ for 18 hours. After incubation the turbidity was checked at absorption of 562 nm. A value of 0.52-0.54 has to be obtained which shows a density of 10^9cells/ml. A dilution of 10^8 organisms was prepared for the experiment. The samples were sterilized in 70% ethanol for 30 minutes and washed once with phosphate buffer saline (PBS). In a 12-well plate, 2ml of culture was added along with the samples and incubated at 37℃ for 24 hours. After incubation, the bacterial culture was removed and the samples were rinsed thrice with PBS. The solution after 3 washes was serial diluted till 10^{-4} dilution. 0.1 ml of 10^{-3} and 10^{-4} dilutions were placed on sterilized nutrient agar (Himedia) plates and incubated at 37° C for 18 hours and the number of bacterial colonies was counted. [9]

RESULTS AND DISCUSSION

Microstructure and Phase Analysis

The *fig.4* shows the surface morphology of as-sprayed AT, YSZ, BL AT/YSZ and BL YSZ/AT hard coatings respectively. The surface morphology of AT coating (*fig. 4.a*) shows fully melted splats with presence of unmelted and partially melted splats. In the case of BL AT/YSZ coating, high degree of fully melted splats with pancake like structures were observed in contrast to the AT coating. This clearly tells us that the underlying YSZ provides better adhesion which leads to the formation of smooth splats. This is reflected from the surface roughness values in which the BL AT/YSZ coating has lower surface roughness due to the smooth splat formation when compared to the AT coating.

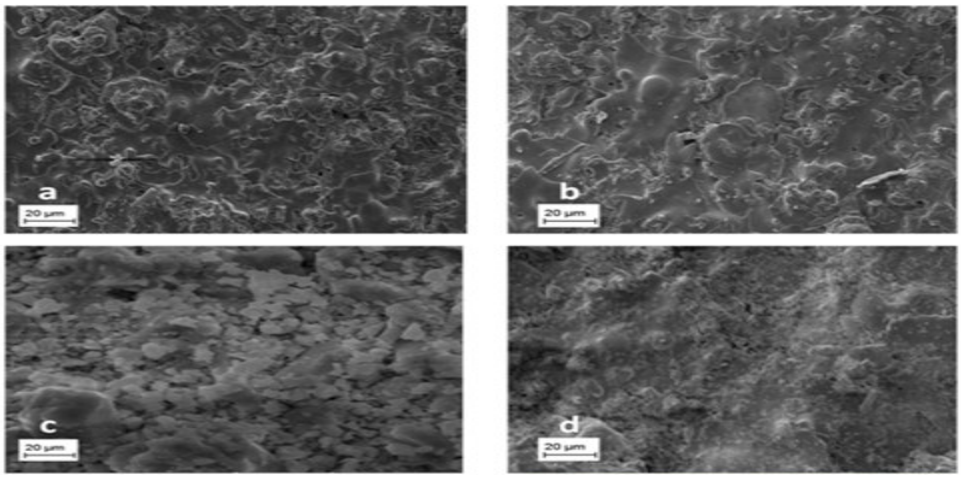

Figure 4
SEM image of the surface of plasma sprayed (a) AT coating (b) YSZ coating (c) BL AT/YSZ coating d) BL YSZ/AT coating

In the YSZ coating, large number of unmelted and partially melted splats were observed rather than fully melted splats. This is due to the mismatch of coefficient of thermal expansion between ZrO_2 ($12x10^{-6}K^{-1}$) and TAV ($8.9x10^{-6}K^{-1}$) alloys. On the contrary, the BL YSZ/AT coating shows large number of fully melted splats with small traces of partially melted and unmelted splats. This is because the coeffient of thermal expansion of the underlying coating i.e., alumina and titania (8 and $7.5x10^{-6}K^{-1}$ respectively) which is similar to that of TAV alloy. From these observations, it can be inferred that the underlying layer influences the surface morphology by inducing high degree of melted splats formation in both the BL AT/YSZ and YSZ/AT coatings. *Fig.5* shows the surface morphology of HaP, TiO_2, 3H7T, 7H3T, 5H5T soft coatings respectively. In the case of HaP coating, large number of unmelted and partially melted splats were observed with high porosity (*table 6)* and in TiO_2 coating, few fully melted splats with predominant amount of unmelted and partially melted splats was seen. On the otherhand, the surface morphology of 3H7T and 7H3T coatings reveals, very few melted particles with higher amount of unmelted and partially melted splats which results in poor bonding between the adjacent splats and a similar observation was by made by Tsui et al., [12]. On the contrary to the above, the equal composition (5H5T) exhibits a higher degree of fully melted splats with trace amount of partially unmelted splats and hence, exhibits less porosity. Thus variation in the formation of melted and unmelted particles in different compositional mixture is due to the difference in melting point of HaP and TiO_2 powders as well as the various concentration and this influences the coating microstructure.

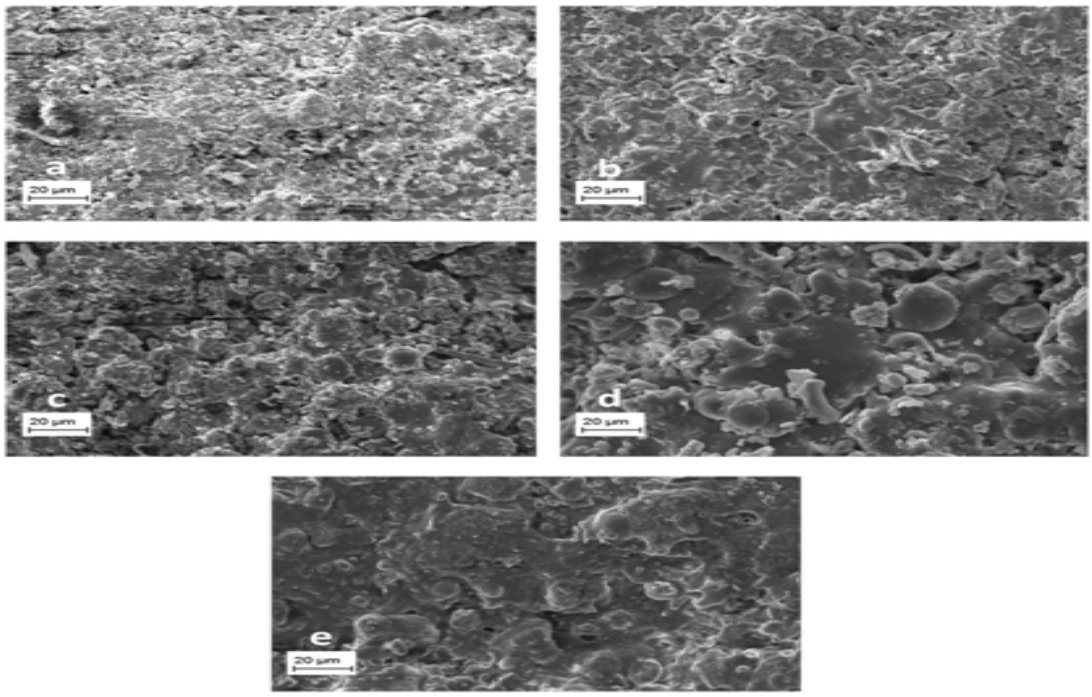

Figure 5
SEM images of Surface of plasma sprayed a) HAP coating b) TiO_2 coating c) 3H7T coating d) 7H3T coating e) 5H5Tcoating

XRD analysis was performed on AT, YSZ, BL AT/YSZ, BL YSZ/AT coatings to study the phase transformation of the powder particles after plasma spray process and it is shown in *fig.6*. In the case of AT coating the presence of $(Al_2Ti)O_5$ phase [JCPDS #81-0030] was observed. BL AT/YSZ coating confirmed the presence of $Al_2Ti_7O_{15}$ phase in accordance with the JCPDS #84-1641. The XRD results for YSZ and BL YSZ/AT shows the presence of combination of Zirconium oxide [JCPDS #89-9069] and Yttrium [JCPDS #12-0702] along with $(Al_2Ti)O_5$ phase in the case of bi-layer coating respectively. It should be noted that a detailed description of the same has been already discussed by *Perumal et.,al.,* [13] [14].

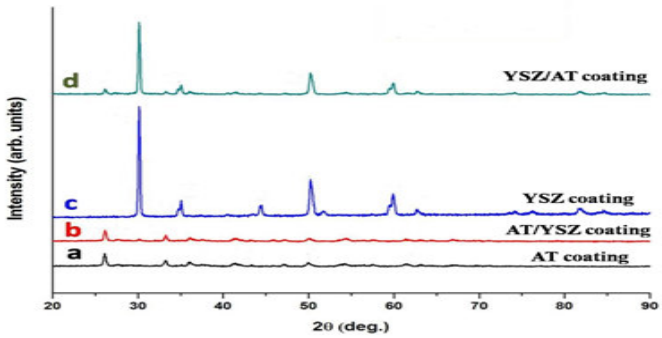

Figure 6
XRD patterns of a) AT coating b) BL-AT/YSZ coating c) YSZ coating d) BL-YSZ/AT coating

In the case of soft coatings, the phases formed in the synthesized HaP, TiO_2 powders and the coatings [HaP, TiO_2, 3H7T, 7H3T, 5H5T] were analyzed and illustrated in *fig. 7*. The phases formed by HaP powder (*fig. 7.a)*, reveals the presence of calcium phosphate which is confirmed with JCPDS#9-432, whereas in HaP coating (*fig. 7.c*) the decomposition of the feedstock resulted in the formation of α-TCP [JCPDS #20-0359] and β-TCP [JCPDS #09-0169] phases. The TiO_2 powder predominantly exhibited the anatase phase along with (110) rutile phase formed at 25° (2θ) (*fig 7.b*) and it is confirmed using JCPDS#84-1286 and JCPDS#88-1175 respectively. In the case of TiO_2 coating [*fig. 7.d*], the anatase phase transformed to rutile phase as the rutile phase is stable at 1100 K [15], compared to the metastable anatase phase. Some researchers have earlier reported the rutile phase formation in the TiO_2 coating at high temperatures, irrespective of the phases formed by the powder [16, 17]. For the composite soft coatings, 3H7T proved to have major TiO_2 phases along with low fractions of HaP. The interaction of TiO_2 acted as a good intermediate in improving the crystalinity of HaP coatings. α and β-TCP at 2θ whereas for 7H3T the TiO_2 phases were suppressed by the α and β-TCP phases with only a single rutile phase observed at 2θ=36°. For 5H5T, the *fig. 7.g* shows high intensity difference at peak positions of 2θ=45 and 53. Along with HaP and TiO_2 phases, the major peaks were almost matching with the standard pattern of $CaTiO_3$ [JCPDS#22-153]. This change might be due to the decompositions of HaP followed by the interaction with TiO_2 leading to the formation of $CaTiO_3$.

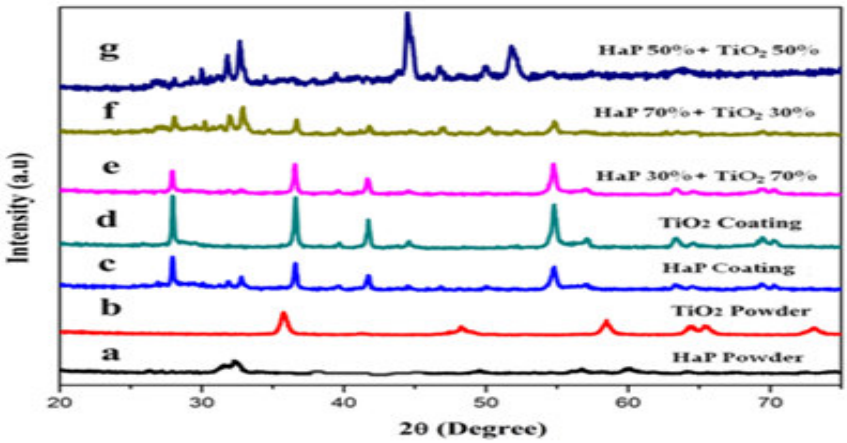

Figure 7
XRD pattern if a) synthesized HaP powder b) synthesized TiO_2 powder c) HaP coating d) TiO_2 coating e) 3H7T coating f) 7H3T coating g) 5H5Tcoating

Hardness

Microhardness measurements were carried out on the cross-section of the coated samples using micro Vickers hardness tester (Chennai Metco). Five measurements were taken, each at a distance of 50 µm (approximately) on both sides of substrate-coating interface. The average micro hardness values of AT, YSZ, BL-AT/YSZ and BL-YSZ/AT coatings are 805±5 HV, 645±4 HV, 1054±53 HV, 1038±41 HV respectively. The variation observed for different coatings is due to the dissimilarity

in microstructure, phase composition and the level of pores and cracks formed in the coating. The highest micro hardness value for the BL-YSZ/AT coating is associated with low porosity in the coating. In the case of soft coatings, the hardness of coatings increased with an increase in TiO_2 content to HaP. The average micro hardness values of HaP, TiO2, 3H7T, 7H3T, 5H5T coatings are 307±9HV, 314±9HV, 381±HV, 354±9HV & 347±HV respectively. The higher hardness value is found to be for 3H7T near the interface which is due to the thermal conductivity of the metallic substrate which acts as a heat sink for the molten particles. The cooling or solidification time for molten HaP particles depends on the thermal conductivity of substrate material and thickness of already deposited lamellae. The solidification time increases with the thickness of lamellae, therefore hardness of coating decreases with an increase in distance from interface or with an increase in coating thickness. Thus the observed difference in hardness between all these coatings is due to the variation in the microstructure, phases present and the volume fractions of pores and cracks [18 19].

Scratch Testing

The scratch test was performed on the plasma sprayed AT, YSZ, BL AT/YSZ and BL YSZ/AT coatings, in order to evaluate the critical load, coating failure and nature of cracks. The scratch result of AT, BL-AT/YSZ and BL-YSZ/AT coating showed long tensile crack on the surface of the coating, whereas the YSZ monolayer coating revealed micro tensile crack, which confirms that all the coatings undergo cohesive failure. Generally, the tensile cracks are formed due to the frictional stress present behind the trailing edge of the stylus and these stresses balance the compressive frictional stresses ahead. [13 20]. Also it is noteworthy to mention that, the substrate was not exposed as the coatings did not spall during the scratch test, which implies that all the coatings has high cohesion strength. Further, the critical load was evaluated for all the coatings and is tabulated in table 3. From the table it is evident that the critical load was higher for BL-YSZ/AT coating. In general, the critical load is a measure at which the coating detaches at certain load. It is obvious that the critical load required is maximum for bilayer coating and this clearly tells that the cohesive strength for this coating is higher when compared to the other coatings. Further, from the *fig.8.a and c*, it is evident that the scratch width is lower for AT coating, which clearly indicates that these coatings posses high cohesive strength.

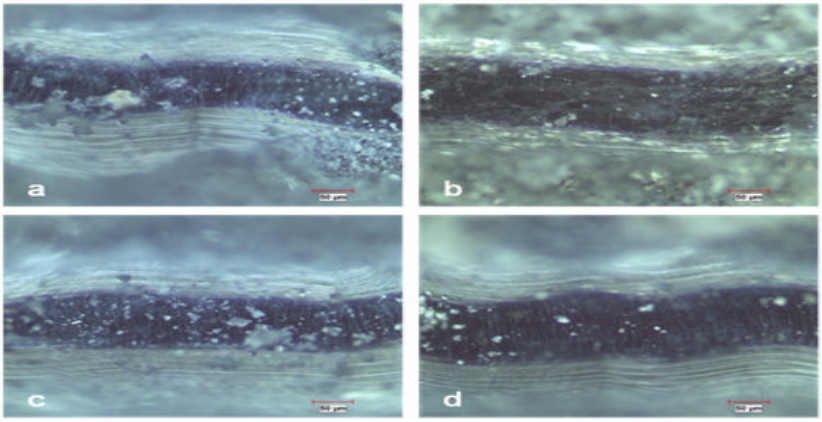

Figure 8
Scratch testing of plasma sprayed (a) AT coating (b) YSZ coating (c) BL AT/YSZ coating d) BL YSZ/AT coating

Table 3
Scratch testing for plasma sprayed AT, YSZ, BL AT/YSZ & BL YSZ/AT coatings

Coating	Critical Load [N]	Nature of Crack	Type of Coating Failure
AT coating	42.75	Long tensile Crack	Cohesive
YSZ coating	45.26	Micro tensile Crack	Cohesive
BL-AT/YSZ coating	48.68	Long tensile Crack	Cohesive
BL-YSZ/AT coating	49.52	Long tensile Crack	Cohesive

The scratch test results of the plasma sprayed HaP, TiO_2, 3H7T, 7H3T, 5H5T coatings are presented in (*fig. 9)* respectively. The scratch morphology of HaP coating showed no tensile crack on the surface, whereas, the TiO_2 coating revealed micro tensile crack with substrate effect, which confirms that this coating has undergone adhesive failure. On the other hand, tensile crack was not observed in 7H3T & 5H5T coatings, while 3H7T coating led to the formation of tensile crack with no substrate effect, resulting in cohesive failure (*table 4)*. These results indicate that HaP, TiO_2, 7H3T & 5H5T coatings adhere weakly to the substrate and hence are unable to withstand higher loads, whereas the 3H7T coatings offer higher resistance to scratch even at higher loads.

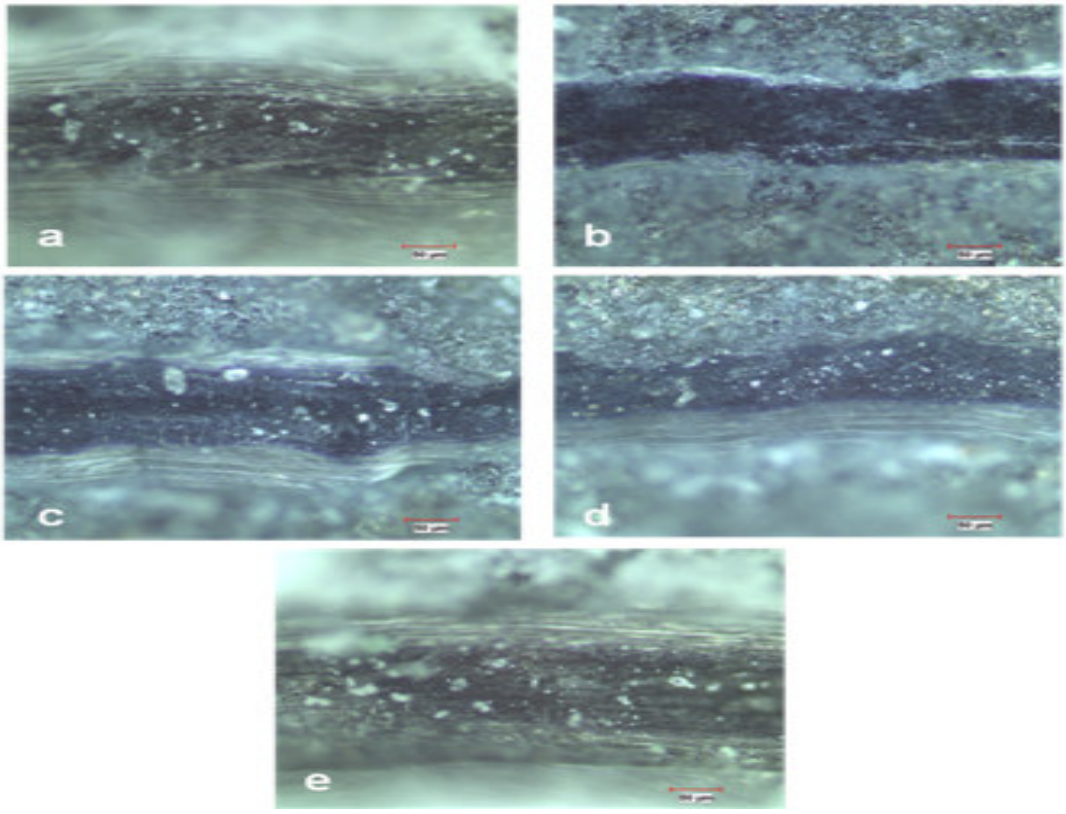

Figure 9
Scratch testing of plasma sprayed (a) HAP coating (b) TiO2 coating 3H7T c) coating d) 7H3T coating e) 5H5Tcoating

Table 4
Scratch testing for plasma sprayed HAP, TiO2, 3H7T, 7H3Tand 5H5Tcoating

Coating	Critical Load [N]	Nature of Crack	Type of Coating Failure
HAP	13.89	No Tensile Crack	Adhesive
TiO2	16.67	Tensile Crack	Adhesive
30%HAP + 70% TiO2	17.94	Long tensile Crack	Cohesive
70% HAP + 30% TiO2	16.96	No Tensile Crack	Adhesive
50%HAP + 50% TiO2	17.48	No Tensile Crack	Adhesive

Wettability & Antibacterial evaluation

Bacteria's are found everywhere and severe infection leading to failure of medical implants will obviously result from surface microbial invasion. Due to the formation of microbes in the implanted site, many failures of implants are widely reported. In order to overcome the problem of failure, implant material should have the capability of antibacterial activity. Hence, the usage of anti-bacterial agent is needed to enhance the life expectancy of the medical implants. However, the usage of antibiotics leads to development of multi-drug resistant strains which posses the major threat to treat infection. Therefore, it is essential to limit the usage of antibiotics. To overcome this, the antibacterial property of various coatings *viz.,* TiO_2, HaP, AT & YSZ was examined. TiO_2 carries positive charge and the *S. aureus* carries negative charge causing electromagnetic attraction leading to free-radical-induced oxidative damage of the cell membranes of bacteria. [21]. Hence, TiO_2 is also extensively used for its antibacterial activity along with HaP to form composite coating. (fig. 12) [22, 23]. From *fig.10*, it is evident that composite coatings exhibited better antibacterial activity than with HaP or TiO_2 alone. The antibacterial activity of the composites were in the order 3H7T>7H3T>5H5T. Hence, 3H7T was found to have the least *S. aureus* colonies showing better antibacterial activity, probably due to higher concentration of TiO_2.

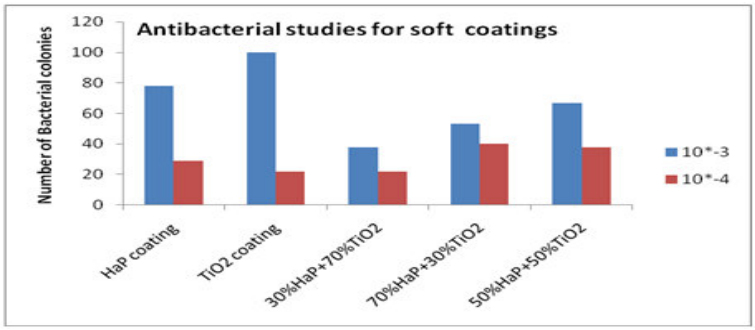

Figure 10
Antibacterial studies for plasma sprayed HaP, TiO2, 3H7T, 7H3T, and 5H5Tcoating

In general, hard coatings comprising of AT, YSZ exhibit less antibacterial activity. Amongst the hard coatings (*fig.11*) the number of bacterial colonies on AT was 29% lesser than YSZ and BL AT/YSZ was 28% lesser than that of BL YSZ/AT. The main factors that influence the bacterial attachment to a biomaterial are found to be different chemical compositions of the material [24] [25], surface potential [26], surface roughness [27] and hydrophilic/hydrophobic property [wettability] [28] [29].

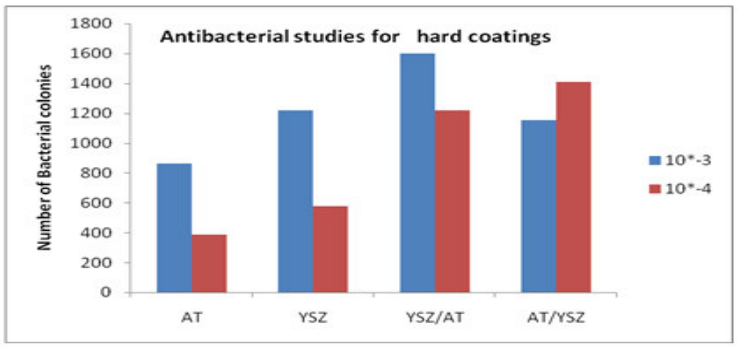

Figure 11
Antibacterial studies for plasma sprayed AT, YSZ, BL AT/ YSZ, BL YSZ/AT coatings

Wettability study involves the measurement of contact angle as the primary data, which basically specifies the degree of wetting property when a solid and liquid interacts. Lower contact angles (<90°) correspond to high wettability, while higher contact angles (>90°) correspond to low wettability. It is also noteworthy to find that the bacteria adhere to materials with varying hydrophobicity, which depends on the hydrophobic property of both material surface and the bacteria [30] [31] [32]. As shown in *fig.12* and *fig.13*, soft coatings exhibited hydrophilicity whereas hard coatings were found to be hydrophobic.

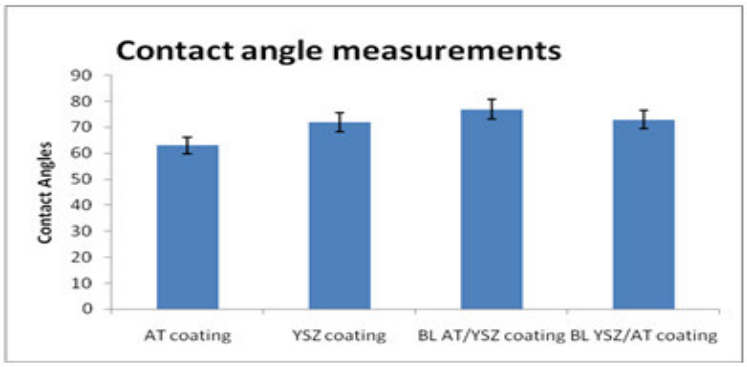

Figure 12
Contact angle measurements for plasma sprayed AT, YSZ, BL AT/YSZ & BL YSZ/AT, coatings

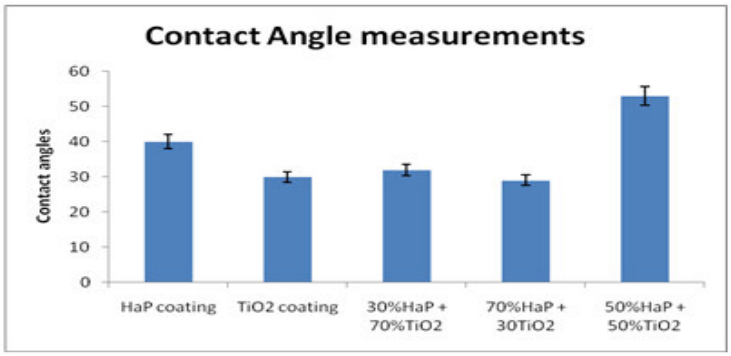

Figure 13
Contact angle measurements for plasma sprayed HAP, TiO2, 3H7T, 7H3T, and 5H5Tcoating

It is evident from the studies performed so far, the soft coatings exhibited enhanced antibacterial activity than hard coatings (*fig. 14 & 15)*, and in addition to wettability factor, the bacterial adhesion is also governed by the surface roughness. The average surface roughness for AT (87°), YSZ (97°), BL AT/YSZ (108°) and BL YSZ/AT (109°) coatings was measured as 6.94µm, 7.85µm, 6.82µm and 7.39µm respectively [*tab. 5]*, and for HaP (40°), TiO_2 (30°), 3H7T (32°), 7H3T (29°), 5H5T (53°) coatings was measured as 5.11µm, 3.06µm, 3.07µm, 3.08µm, 4.38µm respectively (*tab. 6*)

Table 5
Roughness and porosity for plasma sprayed AT, YSZ, BL AT/YSZ & BL YSZ/AT coatings

Coatings	Roughness [Ra]	Porosity [vol%]
AT	6.94µm	13.76
YSZ	7.85µm	13.34
AT/YSZ	6.82µm	11.41
YSZ/AT	7.39µm	11.17

Table 6
Roughness and porosity for plasma sprayed HaP, TiO_2, 3H7T, 7H3T, and 5H5Tcoating

Coatings	Roughness [Ra]	Porosity [vol%]
HaP	5.11µm	11.66
TiO_2	3.06µm	10.45
30%HaP + 70%TiO_2	3.07µm	10.23
70%HaP + 30TiO_2	3.08µm	11.31
50%HaP + 50%TiO_2	4.38µm	10.75

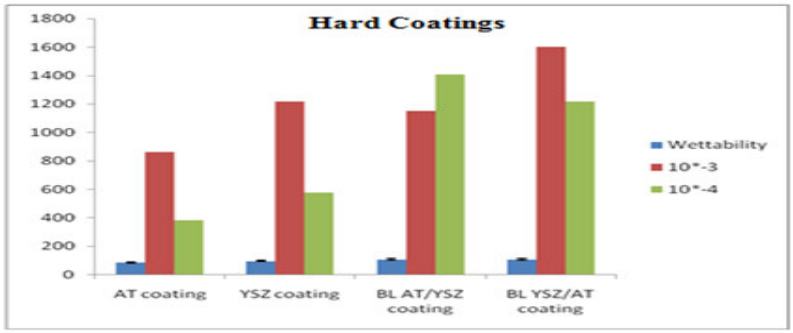

Figure 14
Wettability and antibacterial testing for wear resistant hard coatings

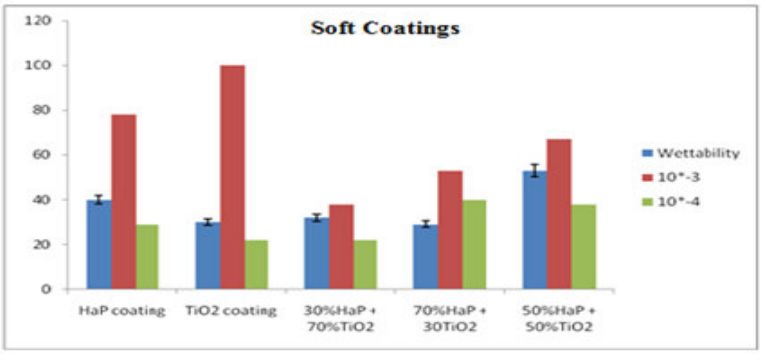

Figure 15
Wettability and antibacterial testing for osseointegration soft coatings

Hence from these results, it is proposed that the surface roughness in the range of 3-5µm with a low contact angle (>55°) prevents adhesion of *S. aureus.* Bunetel *et.al.,* obtained with similar results with increase in roughness through coating process, and a superior increase in the rate of bacterial colonization [33]. From these investigations, it is evident that the surface roughness influences the bacterial adhesion. Prewett *et.al* also indicated that the number of bacterial colonies that adhere to the metal surface is reliant on the bacterial strain and the type of the metal substrate.

CONCLUSION

This work reports on phase analysis, mechanical properties and antibacterial studies on plasma sprayed wear-resistant hard [Alumina Titania-AT, Yttria stabilized Zirconium-YSZ, BL AT/YSZ & BL YSZ/AT] coatings and osseointegration-soft [HaP, TiO_2, 30%HaP+70%TiO_2-3H7T, 70%HaP+30%TiO_2-7H3T, 50%HaP+ 50%TiO_2-5H5T] coatings performed on Ti-6Al-4V alloys for orthopedic applications.

i. The XRD studies performed on the different wear-resistant coatings indeed reveals to be fruitful as it led to the presence of Al_2TiO_5 and $Al_2Ti_7O_{15}$ phases for AT and BL AT/YSZ respectively, and combination of ZrO_2, yttrium along with Al_2TiO_5 phase for YSZ and BL YSZ/AT respectively. On the other hand, for different ratios of osseointegration-soft coatings major phases of rutile TiO_2 and α, β-TCP were found in 3H7T and 7H3T whereas in 5H5T along with TiO_2 and HaP phases, $CaTiO_3$ was also found.
ii. The micro hardness for BL AT/YSZ [1054±53 HV] coating was ~1.3 times higher than AT [805±5 HV] coating and BL YSZ/AT [1038±41 HV] coating was ~1.6 times higher than YSZ [645±4 HV] coating, whereas for different ratio's of HaP/TiO_2 coatings, 3H7T [381±22HV] exhibited slightly higher micro hardness compared to other coatings.
iii. Amongst the various coatings BL YSZ/AT and 3H7T offered higher scratch resistance.
iv. The average surface roughness was in the range of 6-8µm for hard coatings and 3-6µm for soft coatings.
v. Amongst the various wear-resistant hard coatings, AT coating exhibited better antibacterial activity with 29.1% lesser *S. aureus* colonies compared to YSZ coating, 25.1% lesser to BL AT/YSZ coating and 46.1% lesser to BL YSZ/AT coating respectively. Further for osseointegration soft coatings 3H7T was found to have least *S. aureus* colonies which are 28% and 20% lesser than 7H3T and 5H5T respectively.

CONFLICT OF INTEREST

Conflict of interest declared none.

REFERENCES

1. Leela T, Choragudi SF. Antimicrobial Activity Of Nano–Biocomposites For Tissue Engineering Applications. International. Journal of Pharma & Bio Sciences . 2014;5(2):223-32.
2. Pradhaban G, Kaliaraj GS, Vishwakarma V. Antibacterial effects of silver–zirconia composite coatings using pulsed laser deposition onto 316L SS for bio implants. Progress in Biomaterials. 2014 Dec 1;3(2-4):123-30.
3. Busscher HJ, Bos R, Van der Mei HC. Initial microbial adhesion is a determinant for the strength of biofilm adhesion. FEMS microbiology letters. 1995 May 1;128(3):229-34.
4. Zhu H, Guo Z, Liu W. Adhesion behaviors on superhydrophobic surfaces. Chemical Communications. 2014;50(30):3900-13.
5. Braem A, Mellaert L, Mattheys T, Hofmans D, Waelheyns E, Geris L, Anné J, Schrooten J, Vleugels J. Staphylococcal biofilm growth on smooth and porous titanium coatings for biomedical applications. Journal of Biomedical Materials Research Part A. 2014 Jan 1;102(1):215-24.
6. Shen L, Wang B, Wang J, Fu J, Picart C, Ji J. Asymmetric free-standing film with multifunctional anti-bacterial and self-cleaning properties. ACS Applied Materials & Interfaces. 2012 Sep 13;4(9):4476-83.
7. Veerachamy S, Yarlagadda T, Manivasagam G, Yarlagadda PK. Bacterial adherence and biofilm formation on medical implants: a review. Proceedings of the Institution of Mechanical

Engineers, Part H: Journal of Engineering in Medicine. 2014 Oct 1;228(10):1083-99.
8. Hamdi DA, Jiang ZT, No K, Kim JG, Thair L, Jumaae TJ. Investigation The Hydroxyapatite Coatings on Titanium Alloys using Magnetron-Sputtered Process and Differentiate between Single and Triple Layers. Journal of Multidisciplinary Engineering Science and Technology. 2015;2(9).
9. Mathew D, Bhardwaj G, Wang Q, Sun L, Ercan B, Geetha M, Webster TJ. Decreased *Staphylococcus aureus* and increased osteoblast density on nanostructured electrophoretic-deposited hydroxyapatite on titanium without the use of pharmaceuticals. International Journal of Nanomedicine. 2014;9:1775.
10. Mohan L, Durgalakshmi D, Geetha M, Narayanan TS, Asokamani R. Electrophoretic deposition of nanocomposite (HAp+ TiO 2) on titanium alloy for biomedical applications. Ceramics International. 2012 May 31;38(4):3435-43.
11. Park S, Park HJ, Yoo K, Kim HS, Lee JC, Chung YJ, Lee JH, Park MK. Scratch test for immobilization of photocatalytic ZnO nanopowders synthesized by solution combustion method. Journal of Physics and Chemistry of Solids. 2008 Jun 30;69(5):1495-7.
12. Tsui YC, Doyle C, Clyne TW. Plasma sprayed hydroxyapatite coatings on titanium substrates Part 1: Mechanical properties and residual stress levels. Biomaterials. 1998 Nov 30;19(22):2015-29.
13. Perumal G, Geetha M, Asokamani R, Alagumurthi N. Wear studies on plasma sprayed Al_2O_3–40wt% 8YSZ composite ceramic coating on Ti–6Al–4V alloy used for biomedical applications. Wear. 2014 Mar 15; 311(1):101-13.
14. Sathish S, Geetha M, Aruna ST, Balaji N, Rajam KS, Asokamani R. Sliding wear behavior of plasma sprayed nanoceramic coatings for biomedical applications. Wear. 2011 Jun 22;271(5):934-41.
15. Zhao X, Liu X, Ding C, Chu PK. In vitro bioactivity of plasma-sprayed TiO_2 coating after sodium hydroxide treatment. Surface and Coatings Technology. 2006 May 8;200(18):5487-92.
16. Yang GJ, Li CJ, Han F, Ohmori A. Microstructure and photocatalytic performance of high velocity oxy-fuel sprayed TiO 2 coatings. Thin Solid Films. 2004 Nov 1;466(1):81-5.
17. Kucuk A, Berndt CC, Senturk U, Lima RS, Lima CR. Influence of plasma spray parameters on mechanical properties of yttria stabilized zirconia coatings. I: Four point bend test. Materials Science and Engineering: A. 2000 May 31;284(1):29-40.
18. Sarikaya O. Effect of the substrate temperature on properties of plasma sprayed Al_2O_3 coatings. Materials & Design. 2005 Feb 28;26(1):53-7.
19. Sathish S, Geetha M, Aruna ST, Balaji N, Rajam KS, Asokamani R. Studies on plasma sprayed bi-layered ceramic coating on bio-medical Ti–13Nb–13Zr alloy. Ceramics International. 2011 May 31;37(4):1333-9.
20. Hawthorne HM, Xie Y. An attempt to evaluate cohesion in WC/Co/Cr coatings by controlled scratching. Meccanica. 2001 Nov 1;36(6):675-82.
21. Zhang H, Chen G. Potent antibacterial activities of Ag/TiO2 nanocomposite powders synthesized by a one-pot sol− gel method. Environmental Science & Technology. 2009 Mar 18;43(8):2905-10.
22. Fu G, Vary PS, Lin CT. Anatase TiO_2 nanocomposites for antimicrobial coatings. The Journal of Physical Chemistry B. 2005 May 12;109(18):8889-98.
23. Sunada K, Watanabe T, Hashimoto K. Bactericidal activity of copper-deposited TiO_2 thin film under weak UV light illumination. Environmental Science & Technology. 2003 Oct 15;37(20):4785-9.
24. Barth E, Myrvik QM, Wagner W, Gristina AG. In vitro and in vivo comparative colonization of *Staphylococcus aureus* and *Staphylococcus epidermidis* on orthopaedic implant materials. Biomaterials. 1989 Jul 1;10(5):325-8.
25. Oga M, Sugioka Y, Hobgood CD, Gristina AG, Myrvik QN. Surgical biomaterials and differential colonization by *Staphylococcus epidermidis*. Biomaterials. 1988 May 31;9(3):285-9.
26. Hogt AH, Dankert J, Feijen JA. Adhesion of *Staphylococcus epidermidis* and *Staphylococcus saprophyticus* to a hydrophobic biomaterial. Microbiology. 1985 Sep 1;131(9):2485-91.
27. An YH, Friedman RJ, Draughn RA, Smith EA, Nicholson JH, John JF. Rapid quantification of staphylococci adhered to titanium surfaces using image analyzed epifluorescence microscopy. Journal of Microbiological Methods. 1995 Nov 30;24(1):29-40.
28. Reynolds EC, Wong AL. Effect of adsorbed protein on hydroxyapatite zeta potential and Streptococcus mutans adherence. Infection and Immunity. 1983 Mar 1;39(3):1285-90.
29. Pringle JH, Fletcher MA. Influence of substratum hydration and adsorbed macromolecules on bacterial attachment to surfaces. Applied and Environmental Microbiology. 1986 Jun 1;51(6):1321-5.
30. Hogt AH, Dankert J, De Vries JA, Feijen J. Adhesion of coagulase-negative staphylococci to biomaterials. Microbiology. 1983 Sep 1;129(9):2959-68.
31. Satou N, Satou J, Shintani H, Okuda K. Adherence of streptococci to surface-modified glass. Microbiology. 1988 May 1;134(5):1299-305.
32. Fletcher M, Loeb GI. Influence of substratum characteristics on the attachment of a marine pseudomonad to solid surfaces. Applied and Environmental Microbiology. 1979 Jan 1;37(1):67-72.
33. Bunetel L, Segui A, Cormier M, Percheron E, Langlais F. Release of gentamicin from acrylic bone cement. Clinical Pharmacokinetics. 1989 Oct 1;17(4):291-7.